# Comparing the hardness of MAX 2-SAT problem instances for quantum and classical algorithms

Puya Mirkarimi,<sup>1,\*</sup> Adam Callison,<sup>2,3</sup> Lewis Light,<sup>1</sup> Nicholas Chancellor,<sup>1</sup> and Viv Kendon<sup>1,4</sup>

We investigate whether small sized problem instances, which are commonly used in numerical simulations of quantum algorithms for benchmarking purposes, are a good representation of larger instances in terms of hardness. We approach this through a numerical analysis of the hardness of MAX 2-SAT problem instances for various continuous-time quantum algorithms and a comparable classical algorithm. Our results can be used to predict the viability of hybrid approaches that combine multiple algorithms in parallel to take advantage of the variation in the hardness of instances between the algorithms. We find that, while there are correlations in instance hardness between all of the algorithms considered, they appear weak enough that a hybrid strategy would likely be desirable in practice. Our results also show a widening range of hardness of randomly generated instances as the problem size is increased, which demonstrates both the difference in the distribution of hardness at small sizes and the value of a hybrid approach that can reduce the number of extremely hard instances. We identify specific weaknesses that can be overcome with hybrid techniques, such as the inability of these quantum algorithms to efficiently solve satisfiable instances (which is easy classically).

# I. INTRODUCTION

Are the small sized problem instances typically used for numerical simulations actually hard enough to provide a useful test of quantum algorithms? We investigate this question in the setting of continuous-time quantum computing used to solve hard optimization problems. Not all hard problem instances are actually hard, even when they belong to a problem class that is NP-hard. Complexity classes are an asymptotic concept, and even for uniformly NP-hard problem classes, there are easy instances, although they may form a vanishingly small subset in the large size limit. However, for the small sizes we have to use for numerical simulations, the easy instances could form a significant fraction of the instances being processed, and this could significantly skew the results of the simulations.

Despite the above caveats, prior work by some of the authors [1] found surprisingly good scaling for as few as five qubit spin glass ground state problems, using quantum walk computation. This contrasts with the search problem [2, 3], where finite size effects are apparent up to 20 or so qubit problem sizes [4] for all continuous-time quantum computing methods. Crosson et al. [5] identified 20 qubit sized instances of MAX 2-SAT that are hard for quantum annealing (low success probabilities at anneal time T=100). However, this does not guarantee that these instances are also hard for classical algorithms, or for other continuous-time quantum computing methods, such as quantum walk computation.

If different problem instances are harder, or easier, for different algorithms, the best solution method can be a hybrid approach. In this work, we consider the hardness of the MAX 2-SAT instances from [5] for quantum walk computation. We compare these hard instances with typical MAX 2-SAT instances, and also compare the performance of a good classical algorithm. We then evaluate approaches that combine two quantum algorithms and approaches that combine a quantum algorithm and a classical algorithm, to identify hybrid strategies that could outperform a single algorithm used alone.

The paper is organised as follows. In section II, we give an introduction to methods in continuous-time quantum computing and the MAX 2-SAT problem. In section III, we outline the datasets and methods we have used in our numerical analysis. Then, we present the results of our work in section IV, where we make comparisons between the hardness of instances for different algorithms and study the behaviour of these algorithms on satisfiable instances, which are classically easy to solve. Finally, we give an overview of the results and present our conclusions in section V.

### II. BACKGROUND

In this section, we introduce the definitions and concepts used in this work. This includes an overview of continuous-time quantum computing in the coherent regime, a description of the MAX 2-SAT problem, and a mapping of MAX 2-SAT to a problem Hamiltonian. Definitions given in this section will be used when quantifying the success of algorithms in later sections.

<sup>&</sup>lt;sup>1</sup>Department of Physics, Durham University, Durham DH1 3LE, United Kingdom <sup>2</sup>Department of Physics, UCL, Gower Street, London WC1E 6BT, United Kingdom

<sup>&</sup>lt;sup>3</sup> Blackett Laboratory, Imperial College London, London SW7 2BW, United Kingdom

<sup>&</sup>lt;sup>4</sup> Department of Physics, University of Strathclyde, Glasgow G4 0NG, United Kingdom (Dated: June 15, 2022)

<sup>\*</sup> puya.mirkarimi@durham.ac.uk

# A. Continuous-time quantum computing

Continuous-time quantum computing is a model for computing that offers an intuitive approach to solving combinatorial optimization problems on quantum hardware. In this approach, the problem is encoded in a problem Hamiltonian  $H_{\text{problem}}$  such that the ground state of  $H_{\text{problem}}$  corresponds to the desired solution. The computation is performed by initialising a set of qubits to a state  $|\psi(0)\rangle$ , applying a time-dependent Hamiltonian, and measuring the final state of the qubits after a time  $t_f$  has passed. Assuming that the system stays in a fully coherent regime for the full length of the computation, the evolution of the system between the initialisation and measurement steps can be described by the Schrödinger equation. Typically, the Hamiltonian is expressed in the form

$$H(t) = A(t)H_{\text{driver}} + B(t)H_{\text{problem}},$$
 (1)

where A(t) and B(t) are the control functions, which are generally time-dependent, and  $H_{\text{driver}}$  is a Hamiltonian that drives state transitions.

The continuous-time quantum walk (QW) [6] is a form of fully coherent continuous-time quantum computing where the control functions are time-independent. The initial state is chosen to be the ground state of  $H_{\rm driver}$ , which is known in advance and is easy to prepare. The QW Hamiltonian is given by

$$H_{\rm OW}(\gamma) = \gamma H_{\rm driver} + H_{\rm problem},$$
 (2)

where  $\gamma = A(t)/B(t)$  is called the hopping rate. For discussion of the connection between QW and other forms of continuous-time quantum computing, see [1, 4, 7]. QW is a quantum analogue of the classical continuous-time random walk, which is a stochastic process that describes the path of a walker as it takes random steps on a mathematical space. The hopping rate  $\gamma$  can be interpreted as the probability per unit time that the walker will move to an adjacent site.

Another coherent form of continuous-time quantum computing is adiabatic quantum computing (AQC) [8]. In AQC, the system is prepared in the ground state of  $H_{\rm driver}$ , and the Hamiltonian is slowly varied from  $H_{\rm driver}$  to  $H_{\rm problem}$  by varying the control functions from A(0)=1 and B(0)=0 to  $A(t_f)=0$  and  $B(t_f)=1$ . If A(t) and B(t) are monotonically decreasing and increasing respectively and the minimum gap between the energy of the ground state and the first excited state is nonzero, the adiabatic theorem [9] ensures that the system will have a high probability of staying in the instantaneous ground state throughout the computation, provided that the duration of the time-evolution is long enough.

In practice, the problem Hamiltonian is typically expressed as an Ising Hamiltonian on n qubits, which takes

the form

$$H_{\text{problem}} = \sum_{i=1}^{n-1} \sum_{j=i+1}^{n} J_{ij} \sigma_i^z \sigma_j^z + \sum_{i=1}^{n} h_i \sigma_i^z,$$
 (3)

where the couplings  $J_{ij} \in \mathbb{R}$  and field strengths  $h_i \in \mathbb{R}$  are used to encode the problem, and  $\sigma_i^z = \mathbb{1}_2^{\otimes i-1} \otimes \sigma_z \otimes \mathbb{1}_2^{\otimes n-i}$  is the Pauli operator  $\sigma_z$  acting on qubit i and identities acting on all other qubits. A common choice for the driver Hamiltonian in both QW and AQC is the transverse field Hamiltonian

$$H_{\text{driver}} = -\sum_{i=1}^{n} \sigma_i^x,\tag{4}$$

where  $\sigma_i^x$  is defined similarly to  $\sigma_i^z$  as  $\sigma_i^x = \mathbb{1}_2^{\otimes i-1} \otimes \sigma_x \otimes \mathbb{1}_2^{\otimes n-i}$ . The ground state of this driver Hamiltonian, which in QW and AQC is the initial state of the system, is the equal superposition of the computational basis states,

$$|\psi(0)\rangle = \frac{1}{\sqrt{2^n}} \sum_{j=0}^{2^n - 1} |j\rangle = |+\rangle^{\otimes n},$$
 (5)

where  $|+\rangle = (|0\rangle + |1\rangle)/\sqrt{2}$ .

Whereas in AQC one can always attain a near-unity probability of successfully measuring the state corresponding to the optimal solution by using a long enough run time, in QW the probability of success does not generally approach unity, regardless of the run time. Therefore, to find the optimal solution with a probability of close to unity using QW, one should perform the computation many times and take the best found solution. For simplicity, in the rest of this work we will only be considering problem instances that have a unique optimal solution corresponding to a non-degenerate ground state  $|G\rangle$  of the problem Hamiltonian. The probability of measuring the state  $|G\rangle$  after evolving the system for a time  $t_f$  is

$$P(t_f) = \left| \langle G | \psi(t_f) \rangle \right|^2. \tag{6}$$

In general, the success probability  $P(t_f)$  for QW fluctuates with time in an unpredictable manner. To avoid taking every measurement at a time when  $P(t_f)$  happens to be near a local minimum, it is beneficial to use different values of  $t_f$  for each measurement. We will consider the approach of selecting  $t_f$  uniformly at random from an interval  $[t, t + \Delta t]$ . We define the average single run success probability as

$$\overline{P}(t, \Delta t) \equiv \frac{1}{\Delta t} \int_{t}^{t+\Delta t} P(t_f) dt_f, \qquad (7)$$

which is the mean success probability of individual measurements in this approach. The number of repeats required to attain an arbitrarily high probability of measuring the ground state scales as the inverse of  $\overline{P}(t, \Delta t)$  for small  $\overline{P}(t, \Delta t)$ .

For both QW and AQC, the choice of control functions is a free parameter that can affect the performance of the algorithms. In QW, this corresponds to the hopping rate  $\gamma$ . A good choice for  $\gamma$  is one that balances the energy between  $H_{\text{driver}}$  and  $H_{\text{problem}}$  in the total Hamiltonian [1]. To achieve this, we would like to set  $\gamma$  such that the energy-spread of  $\gamma H_{\text{driver}}$  is equal to the energy-spread of  $H_{\text{problem}}$ . For the transverse-field driver Hamiltonian defined in Eq. (4), the energy-spread is  $2n\gamma$ . However, the energy-spread of the problem Hamiltonian depends on the particular problem instance, and it is not possible to calculate it without solving the instance. Therefore, we instead consider the average energy-spread  $\langle s_{\text{problem}} \rangle$ of  $H_{\text{problem}}$  for instances of a given number of variables n, and we calculate a heuristic hopping rate  $\gamma_{\text{heur}}$  by setting this equal to the energy-spread of  $H_{\text{driver}}$ , giving

$$\gamma_{\text{heur}} = \frac{\langle s_{\text{problem}} \rangle}{2n}.$$
(8)

For our analysis, the average energy-spread  $\langle s_{\text{problem}} \rangle$  was calculated for each n by diagonalising the problem Hamiltonians of the generated instances (i.e., solving the problems). In practice, when the size of the instances makes this approach too computationally expensive,  $\langle s_{\text{problem}} \rangle$  can be calculated for similar instances with fewer variables and extrapolated to larger n.

The choice of control functions that we have used for all AQC simulations in this analysis is the linear schedule

$$A(t) = 1 - \frac{t}{t_f}, \ B(t) = \frac{t}{t_f}.$$
 (9)

While there exist strategies involving QW and AQC with different choices of control functions that can improve performance [10], we will not be exploring them in this work. The simulations in [5] used the same linear schedule as above with a constant duration  $t_f = 100$ , which is close to the adiabatic limit for most of the randomly generated instances at the chosen size. (Over half of the instances had success probabilities of P(100) > 0.95.) However, the instances that were selected for being hard had success probabilities of  $P(100) < 10^{-4}$ , which puts their simulations far from the adiabatic limit. Hence, these instances are hard for a specific quantum annealing (QA) protocol that relaxes the condition of adiabacity in AQC.

### B. MAX 2-SAT

A Boolean formula  $\phi = \phi(x_1, \dots, x_n)$  consists of n Boolean variables  $x_1, \dots, x_n$ , Boolean operators, and parentheses. The Boolean operators we will consider are conjunction  $(\land)$ , disjunction  $(\lor)$ , and negation  $(\neg)$ . Boolean variables can take one of the two possible logical values true (denoted 0) and false (denoted 1). A set of values that are assigned to the n variables in a formula is called an assignment, and for each assignment the

Boolean formula  $\phi$  will evaluate to either true or false. We define 2n literals  $l_1, \ldots, l_n$  and  $l_{-n}, \ldots, l_{-1}$  such that the literal  $l_i$  is associated with the variable  $x_i$  if i is positive, or  $\neg x_{|i|}$  if i is negative.

In the maximum satisfiability problem (MAX SAT), a problem instance is specified by a Boolean formula  $\phi$  that is in conjunctive normal form (CNF), which is a formula that is structured as a conjunction of m clauses, where a clause is a disjunction of literals. In this work, we will be studying maximum 2-satisfiability (MAX 2-SAT), which is a special case of MAX SAT where there are two literals in each clause. An example of a valid formula for MAX 2-SAT is

$$(x_1 \lor x_2) \land (\neg x_1 \lor x_2) \land (x_1 \lor \neg x_3) \land (\neg x_1 \lor x_3) \land (\neg x_2 \lor x_3) \land (\neg x_2 \lor \neg x_3),$$

$$(10)$$

where n=3 and m=6 in this case. In MAX 2-SAT, any possible truth assignment is known as a solution, and we are tasked with finding an optimal solution, which is a solution that maximises the number of clauses that evaluate to true. A clause that evaluates to true is said to be satisfied, and a clause that evaluates to false is said to be unsatisfied. The formula above has four optimal solutions which each satisfy five of the six clauses, one of which is the assignment  $x_1=0,\ x_2=0,\ x_3=0$ .

Although 2-SAT, the decision version of MAX 2-SAT, is in the complexity class P, MAX 2-SAT is NP-hard. Nevertheless, MAX SAT solvers have made remarkable advancements over the past three decades, and they are able to solve or approximately solve MAX 2-SAT instances with relatively large input sizes. This progress can in part be attributed to annual competitions in producing the fastest SAT and MAX SAT solvers [11, 12] and the large demand for these solvers, which is generated from the ability to efficiently map a wide range of practical problems to satisfiability problems. Examples include software verification [13, 14], planning [15, 16], and design debugging [17, 18].

In this paper, we will be using the word "hard" to refer to both a hard instance and a hard problem with different meanings. The hardness of an instance refers to the amount of resources used by a given algorithm to solve the instance, relative to other instances of the same problem size. An instance that is hard for one algorithm may not necessarily be hard for another algorithm. The hardness of a problem refers to the amount of resources used by all possible instances of a given size, typically measured by the worst-case or average-case computational complexity. Due to MAX 2-SAT being NP-hard, we expect a worse than polynomial scaling of the worst-case time complexity with n for any algorithm.

In practice, the average run time scaling for a given set of instances may differ significantly from the worstcase time complexity of the problem and may be polynomial, even if the problem is NP-hard. The way in which instances are sampled is often an important consideration when performing an analysis on run times, especially when the problem is not uniformly hard. It has been shown that the hardness of MAX 2-SAT instances increases with the clause density  $\rho=m/n$ , and that there is a hardness phase transition at the critical clause density  $\rho_c=1$  [19, 20]. This has been demonstrated experimentally for QA [21].

#### C. Problem mapping

In order to solve instances of MAX 2-SAT with a continuous-time quantum algorithm, a mapping of the problem as a Hamiltonian in the form given by Eq. (3) is required. Such a mapping should assign lower energies to eigenstates corresponding to more optimal solutions. Under the binary encoding of Boolean variables  $x_i \in \{0,1\}$  where 0 corresponds to true and 1 corresponds to false, the disjunction operator is equivalent to multiplication—i.e.  $x_i \vee x_j$  can be written as  $x_i x_j$ . By identifying the variable  $x_i$  with the single-qubit basis state  $|x_i\rangle$ , we observe that

$$\frac{1 - \sigma_z}{2} |x_i\rangle = x_i |x_i\rangle, \qquad (11)$$

where  $\sigma_z$  is the Pauli Z operator. For a clause  $C_k = l_i \vee l_j$ , where the literal  $l_i$  is positive (negative) if the number i is positive (negative), the corresponding term in the problem Hamiltonian can be constructed by taking the product

$$H_{C_k} = \frac{1 - \operatorname{sgn}(i)\sigma_{|i|}^z}{2} \frac{1 - \operatorname{sgn}(j)\sigma_{|j|}^z}{2}, \quad (12)$$

where we have used the sign function sgn to extract the sign of the indices. This term contributes an energy equal to  $x_i x_j$ . The problem Hamiltonian can then be constructed by taking a sum over the terms corresponding to each of the clauses in the Boolean formula  $\phi$ , giving

$$H_{\text{problem}} = \sum_{C_k \in \phi} H_{C_k}.$$
 (13)

The eigenvalues of this Hamiltonian are equal to the numbers of clauses that are unsatisfied by the assignments corresponding to the eigenstates.

# III. NUMERICAL METHODS

#### A. Datasets

We performed our numerical study on two sets of MAX 2-SAT instances. The first set of instances were generated by Crosson et al. in [5], and each instance in this set contains n=20 Boolean variables and m=60 clauses. Having a constant clause density  $\rho=3$  that is well above the critical clause density ensures that these instances are in the hard regime. Each of the clauses in these instances were generated by randomly selecting

two literals that are associated with distinct variables. Instances with multiple optimal solutions (corresponding to degenerate ground states of the problem Hamiltonian) were discarded. 202,078 of such instances were generated, but only those with an AQC success probability at time  $t_f=100$  of  $P(100)<10^{-4}$  were selected, meaning that the 137 instances that remained are hard for QA. For convenience, these instances were transformed by negating all literals corresponding to variables that were set to 1 in the original optimal assignment so that the optimal solution is always the  $00\dots0$  bit string.

The second set of instances were generated in a similar manner as those from [5]. For each number of variables in the range  $5 \le n \le 20$ , 10,000 instances containing m = 3n unique clauses were generated with randomly selected pairs of literals corresponding to distinct variables for each clause, and only the instances with unique optimal solutions were kept. The transformation to set 00...0 as the optimal solution was applied. Unlike the instances from [5], there was no post-selection of a fraction of these instances based on hardness; hence, we will refer to these as the "typical" instances. It has been shown that instances with an unbalanced ratio of positive to negative literals (or unnegated to negated variables) may be harder than balanced instances, where there are an equal number of positive and negative literals [22]. These instances are on average balanced and hence aren't maximally hard.

#### B. Numerical tests

All of the findings in this paper are results of numerical simulations that were carried out using the Python programming language [23]. The NumPy [24] and Scipy [25] libraries were used for computationally intensive calculations, and matplotlib [26] was used for plotting. The implementation of the least-squares method in scipy.optimize.curve\_fit was used for obtaining the linear fits in this paper. The unitary time-evolutions of quantum systems were simulated using quimb [27] as a convenient interface to scipy.integrate.complex\_ode and its implementation of dop853 [28], which is a Runge-Kutta method of order 8 with an adaptive step-size. Simulations were run on the high performance computers at Imperial College London.

The quantity of interest for our analysis of QW is the average single run success probability  $\overline{P}(t,t+\Delta t)$  given in Eq. (7), which is defined over an interval of measurement times  $[t,t+\Delta t]$ . We set t=0 and  $\Delta t=100$  for our calculations, which produces an interval that is longer than the timescale of the QW dynamics. To demonstrate this, we plot the instantaneous QW success probability in this interval for pairs of randomly selected instances with n=5 and n=20 variables in Fig. 1, and we see that there are many oscillations in the success probability within the time interval in each case. The average success probability  $\overline{P}(0,100)$  was approximated by numerically inte-

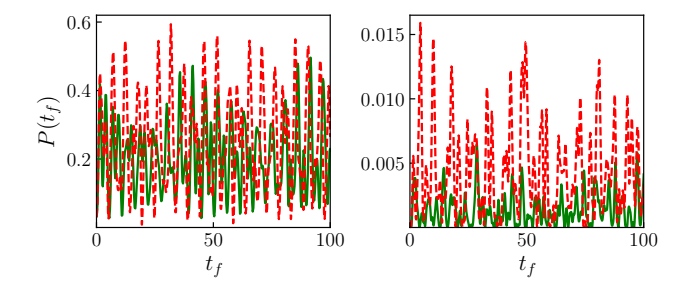


FIG. 1. Instantaneous QW success probability  $P(t_f)$  for two randomly selected pairs of instances (solid green and dashed red lines) with n=5 variables (left) and n=20 variables (right) plotted against measurement time  $t_f$ . Note the difference in the upper limits of the y-axes.

grating the Schrödinger equation over the full time interval and taking a weighted average of the instantaneous success probabilities of the solutions that were evaluated at each iteration of the integration method, where the weights are given by the amount of time between successive iterations.

For AQC, the quantity of interest is the minimum evolution duration required to achieve a 99% success probability  $T_{0.99}$ . To find  $T_{0.99}$  for a given instance, the quantum dynamics were simulated for a small duration Tand the success probability was calculated according to Eq. (6). If the success probability was less than 99%, the duration was doubled and a new success probability was calculated. This was repeated until either a success probability of greater than 99% was found or the simulations became too computationally intensive to continue, in which case  $T_{0.99}$  was not found. If the original success probability was greater than 99%, the duration was instead halved each time until a duration with less than 99% success probability was found. The bisection method was then used to search for  $T_{0.99}$  up to a desired precision within the interval of the last two durations.

The classical algorithm MixBandB [29] was applied to all of the generated MAX 2-SAT instances in order to compare its performance to the quantum algorithms. MixBandB was written to mirror some of the key characteristics of a highly competitive MAX SAT solver known as MIXSAT [30], without including many of the heuristic methods that MIXSAT employs. Like MIXSAT, MixBandB is a branch-and-bound algorithm that uses the "Mixing method" [31] as a semidefinite programming solver in order to produce lower bounds, and rounding to produce good guesses. MixBandB does not use a dual initialisation strategy or any of the data structure or implementation optimizations that are present in MIXSAT. For each instance, we measured the number of times MixBandB accessed the problem specification, which we refer to as the number of problem calls  $N_{\text{calls}}$ . This quantity serves as a proxy for the run time of the algorithm.

#### IV. RESULTS

In this section, we present an analysis of the hardness of MAX 2-SAT instances for various quantum and classical algorithms based on the results of numerical simulation. The QW success probability  $\overline{P}(0, 100)$  is used as a measure of the hardness of instances for QW, where a higher success probability corresponds to an easier instance, and the AQC duration  $T_{0.99}$  is used as a measure of hardness of instances for AQC, where a longer duration corresponds to a harder instance. We start by making a cross-comparison between the hardness of MAX 2-SAT instances for QW and AQC in section IVA, and we make further comparisons that include hardness for a good classical algorithm in section IVB. Where we were able to obtain results for 20-variable instances, a comparison with QA hardness using the instances from [5] is also made. In section IV C, we quantify the relative hardness of satisfiable instances, which are classically easy to solve, for the algorithms that we are considering.

# A. QW/AQC hardness comparison

To characterise the relation between the QW hardness and AQC hardness of MAX 2-SAT instances, Fig. 2 shows the joint distribution between  $\overline{P}(0,100)$  and  $T_{0.99}$  for typical instances with n=5 variables and n=15 variables—the latter being the largest problem size that we could calculate  $T_{0.99}$  for. We calculate the Spearman's rank correlation coefficient for the distribution to be  $\approx 0.04$  and  $\approx -0.71$  for n=5 and n=15 respectively. This indicates a correlation between QW and AQC hardness that gets stronger with increasing n, and it suggests that while a hybrid strategy may be able reduce the total run time, it would not produce a massive improvement at larger problem sizes, as the instances that are hard for one algorithm aren't likely to be found easy by the other algorithm.

In the bottom plot of Fig. 2, a long tail of instances that are extremely hard for both QW and AQC can be identified visually. These instances are towards the top-left of the heatmap and are far from the location where the heatmap shows the highest density of instances. In comparison, the tail of instances to the bottom-right of the heatmap is much shorter, indicating that there aren't as many outlying easy instances as there are outlying hard instances for both QW and AQC. It is possible that typical instances of this problem size are more dominated by easy instances than what would be found at larger problem sizes. In other words, the top and left sides of the graph may have a higher density of instances when plotted for larger n, due to there being more instances in the "hard tail" of the distribution. If this were the case, then the hardest of the typical instances may be a better representation of the types of instances that are typically found at larger problem sizes. On top of this, instances of practical interest may have a significantly

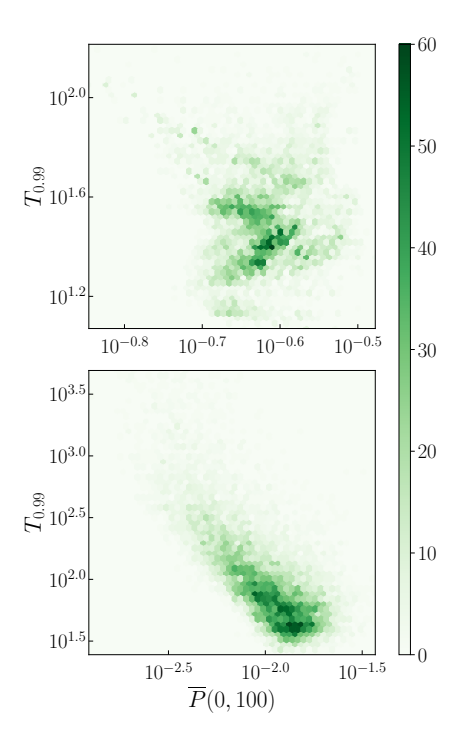


FIG. 2. Heatmaps of the AQC duration  $T_{0.99}$  against the QW success probability  $\overline{P}(0,100)$  for typical MAX 2-SAT instances with n=5 variables (top) and n=15 variables (bottom), excluding 132 instances of size n=15 for which  $T_{0.99}$  was not successfully calculated. Visually, the bottom plot looks reasonably well correlated, whereas the top plot does not appear to show much correlation. This is confirmed by the Spearman's rank correlation coefficients, which were calculated to be  $\approx 0.04$  for n=5 and  $\approx -0.71$  for n=15.

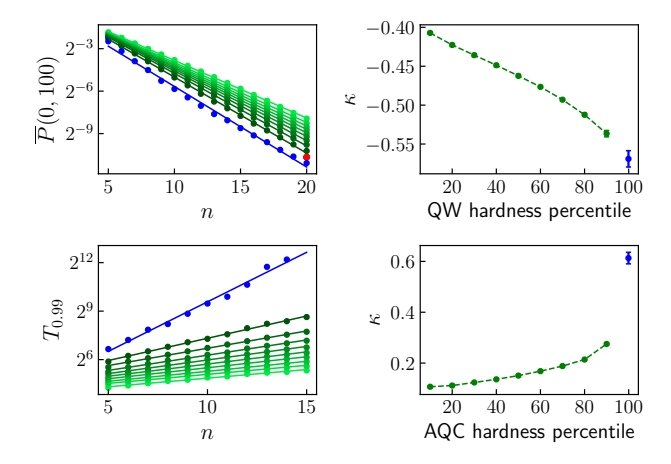
different composition of harder and easier instances than our sample of randomly generated instances. Therefore, it would be useful to find out whether the level of correlation between  $\overline{P}(0,100)$  and  $T_{0.99}$  changes with the hardness of the instances, but this is difficult to tell from these heatmaps.

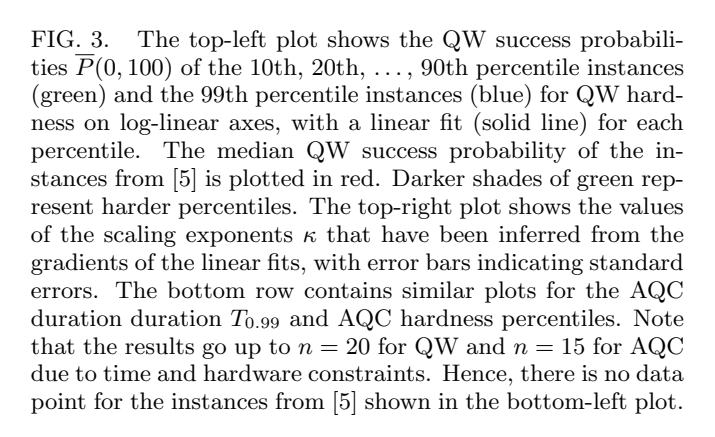
A more detailed analysis of the hardness of instances is required to distinguish between the increase in hardness with n that is simply due to the increase in problem size from the change in the distribution of the hardness of the instances for QW and AQC at each n. This is difficult to achieve because we expect the proportion of very hard instances to increase with n. To accommodate such an analysis, we have grouped the typical instances of each number of variables n into deciles, ranking them by hardness. Decile 1 contains the easiest 10% of the instances, decile 2 contains the next easiest 10% of the instances, and so on, with decile 10 containing the hardest 10% of the instances. This partitioning is done using the average QW success probability  $\overline{P}(0, 100)$  as the measure of hardness to produce "QW hardness deciles" and similarly done using the 99% success probability duration  $T_{0.99}$  for AQC to produce "AQC hardness deciles". For AQC, it is assumed that the instances that we were not able calculate  $T_{0.99}$  for in a reasonable amount of time are the hardest instances. To identify the very hardest instances, we have also grouped together the hardest 1% of instances at each n for QW and for AQC using the same measures of hardness as for the deciles. By defining the QW/AQC "hardness percentiles" in a similar way as the hardness deciles, we can refer to the instances that are on the boundaries of the deciles by their percentiles. For example, the hardest instance in the 3rd QW hardness decile is the 30th percentile instance for QW hardness. Similarly, the hardest instance for AQC that is not one of the hardest 1% of instances for AQC is the 99th percentile instance for AQC hardness.

The top-left of Fig. 3 shows a log-linear plot of the average success probabilities  $\overline{P}(0,100)$  for the hardest instances of each QW hardness decile (excluding the hardest decile) and the 99th percentile instances for QW hardness against the number of variables n. A linear fit is shown for each of the decile boundary instances and the 99th percentile instances, and the corresponding scaling exponents for each fit are plotted on the top-right. These plots show that the scaling of  $\overline{P}(0, 100)$  gets progressively worse as the subset of selected instances gets harder. Therefore, at larger problem sizes we can expect a bigger difference between the hardness of the easiest and the hardest instances. The inferred scaling exponents also indicate that the tail of hard instances gets longer as n is increased, which means that the time spent solving many instances would be largely dominated by the hardest instances. This highlights the value of a hybrid approach, as any efficiency improvement for the hardest instances would make a significant difference to the total run time.

A red point indicating the median value of  $\overline{P}(0, 100)$ for the instances from [5] is shown in the top-left of Fig. 3. The placement of this point shows that these instances are also hard QW, which suggests that there is a correlation between QW and QA hardness. These instances were selected to be the hardest 147 instances for QA out of 202,078 randomly generated instances, meaning that the median instance that we have plotted is approximately the 99.9th percentile instance for QA hardness. However, the QW hardness of this instance lies between the 90th and 99th percentiles of the typical instances, which indicates that the instances from [5] are not as extremely hard for QW as they are for QA. Given that these instances are at least four orders of magnitude harder for QA than the median of the randomly generated instances, their lower relative hardness for QW is substantial, and an approach involving QA would benefit from speeding up these instances by running QW in parallel.

The bottom row of Fig. 3 shows similar plots as above, but this time for the AQC duration  $T_{0.99}$  and AQC hardness deciles/percentiles. The median value of  $T_{0.99}$  for the instances from [5] was not calculated, as these instances were too large to run AQC simulations for. Just as with the QW results, we find that harder percentiles scale more harshly for AQC, and this effect is even more prominent than for QW. (The decile boundary scaling ex-





ponents range from  $\kappa = 0.107 \pm 0.004$  to  $\kappa = 0.275 \pm 0.005$ for AQC, as opposed to  $\kappa = -0.407 \pm 0.002$  to  $\kappa =$  $-0.537\pm0.004$  for QW.) Notably, there is a large jump in the value of  $T_{0.99}$  between the 90th and 99th percentile instances, which implies that a small subset of the instances we are considering are extremely hard for AQC. This is not surprising, as it is known that AQC performs very poorly on instances of other NP-hard problems when the minimum energy gap between the ground and first excited states is extremely small [32]. The steep gradient of the fit for the 99th percentile instances may be an indication that the number of extremely hard instances is growing with n, which would be consistent with the idea that we would see a larger fraction of instances in the "hard tail" at larger n. Therefore, we are further motivated to analyse the relation between QW and AQC hardness for these extremely hard instances.

To make a cross-comparison between QW and AQC, we examine the QW hardness of instances when grouped by AQC hardness, and vice versa. In the top-left of Fig. 4, we plot the median values of the QW success probability  $\overline{P}(0,100)$  for the instances in each AQC hardness decile against n on log-linear axes. The median values of  $\overline{P}(0,100)$  for the hardest 1% of instances for AQC are also plotted. A straight line is fit to the points for each of these groups of instances, and the corresponding scaling exponents are plotted in the top-right of the figure.

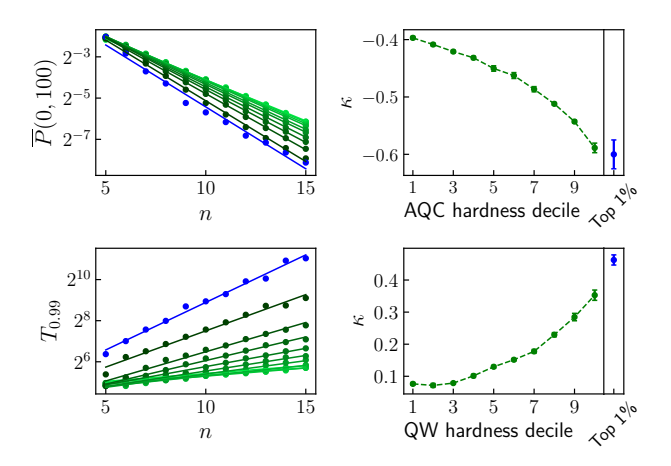


FIG. 4. The top-left plot shows the median value of the QW success probability  $\overline{P}(0,100)$  of each of the AQC hardness deciles (green) and the hardest 1% of instances for AQC (blue) on log-linear axes, with a linear fit (solid line) for each category. Darker shades of green represent harder deciles. The top-right plot shows the values of the scaling exponents  $\kappa$  that have been inferred from the gradients of the linear fits, with error bars indicating standard errors. The bottom row contains similar plots for the median values of the AQC duration  $T_{0.99}$  for instances organised by QW hardness.

The fact that harder AQC deciles tend to correspond to smaller median values of  $\overline{P}(0, 100)$  implies that AQC hardness is a good indicator of QW hardness. Note that this is not the case at the lowest values of n, but the correlation becomes more clear as n is increased. This agrees with the correlations we found in Fig. 2. The implied scaling exponents show that this increase in QW hardness with AQC hardness becomes more prominent across all of the deciles as n is increased. In particular, the correlation between QW hardness and AQC hardness seems to remain strong at the "hard tail" of the distribution. However, there isn't a large jump in the scaling for the hardest 1% of instances for AQC on QW, which shows that the extremely hard instances for AQC aren't as extremely hard for QW. This indicates an advantage of the hybrid strategy for solving the instances that AQC finds extremely hard.

We make a similar comparison in the bottom row of Fig. 4, where we plot the median AQC durations  $T_{0.99}$ , and the corresponding scaling exponents, for the instances in QW hardness deciles and the 99th percentile instances for QW hardness. In accordance with the previous results, these plots indicate that QW hardness is a good indicator of AQC hardness, though this is again more clearly the case for larger n. The trend of worsening scaling exponent with increasing hardness decile in both sets of comparisons indicates that the QW-AQC hardness correlation is likely to continue to larger n, even for the tail of hard instances. Therefore, a simple hybrid strategy is unlikely to produce a drastic speedup, though there is still room for some speedup, especially for the in-

stances that are extremely hard for AQC. Assuming that performing runs of QW and AQC incurs a cost of roughly a factor of two to the total run time, even a small scaling advantage obtained from this approach would make up for this cost at large problem sizes.

#### B. Quantum/classical hardness comparison

To quantify the classical hardness of MAX 2-SAT instances, we have measured the number of problem calls  $N_{\rm calls}$  made by the classical algorithm MixBandB when solving each MAX 2-SAT instance. While there exist many classical algorithms that perform much better than MixBandB, they tend to employ heuristic methods to gain a speed advantage, which make a significant difference at small problem sizes. This is undesirable for our analysis because the quantum algorithms we are comparing them to do not use such heuristics. MixBandB is based on MIXSAT, which is a powerful MAX SAT solver, but it does not incorporate the heuristic optimizations that MIXSAT uses. In this sense, MixBandB is a good classical comparison to QW and AQC. However, MixBandB is an exact solver, meaning that it always returns an optimal solution at the end of a run, whereas QW and AQC cannot give such guarantees. Since the purpose of this work is not to benchmark the scalings of these algorithms, this difference is not important for our analysis.

Fig. 5 shows a histogram of the approximate probability density of the logarithm of the number of calls  $N_{\text{calls}}$ made by MixBandB for typical instances with n=20variables and the instances that are hard for QA. It can be seen that the typical instances form a bimodal distribution, where there is a peak of instances that required relatively few calls, and a long tail of harder instances that form another peak at a higher number of calls. This suggests that the typical instances can be roughly divided into classically hard and easy categories, with the majority of instances being easy. The instances that are hard for QA also form a bimodal distribution, but with a larger peak of hard instances than easy instances. The centre of this distribution is located on the "hard tail" of typical instances, suggesting that hard instances for QA tend to be hard for MixBandB too.

In Fig. 6, we plot the joint distribution of  $N_{\rm calls}$  and  $\overline{P}(0,100)$  for the typical instances with n=15 variables, and the joint distribution of  $N_{\rm calls}$  and  $T_{0.99}$  for the 9868 typical instances that we successfully calculated  $T_{0.99}$  for. The former distribution has a Spearman's rank correlation coefficient of  $\approx -0.47$ , and the latter has a Spearman's rank correlation coefficient of  $\approx 0.52$ . These imply that correlations exist between hardness for MixBandB and hardness for both QW and AQC, although the correlations are not as strong as what we previously observed between QW hardness and AQC hardness at the same problem size. Therefore, it seems that a hybrid strategy would be more effective when applied to a quantum

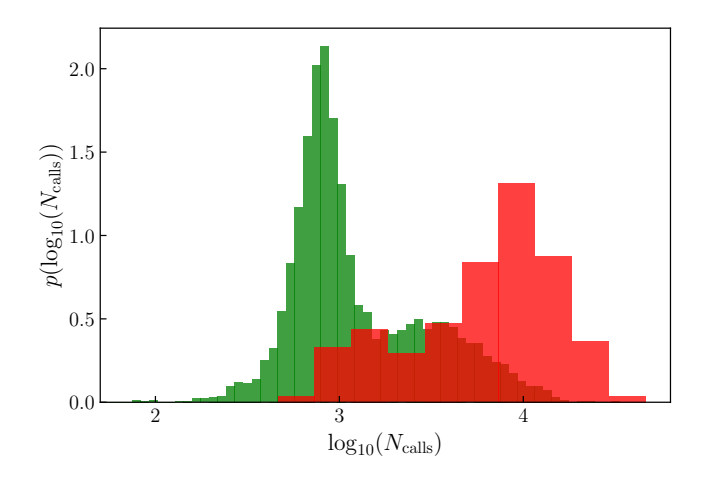


FIG. 5. Histogram showing the approximate probability density  $p(\log_{10}(N_{\text{calls}}))$  of the logarithm of the number of problem calls  $N_{\text{calls}}$  made by the MixBandB algorithm when solving the typical n=20 instances (green) and the instances from [5] (red), which are hard for QA.

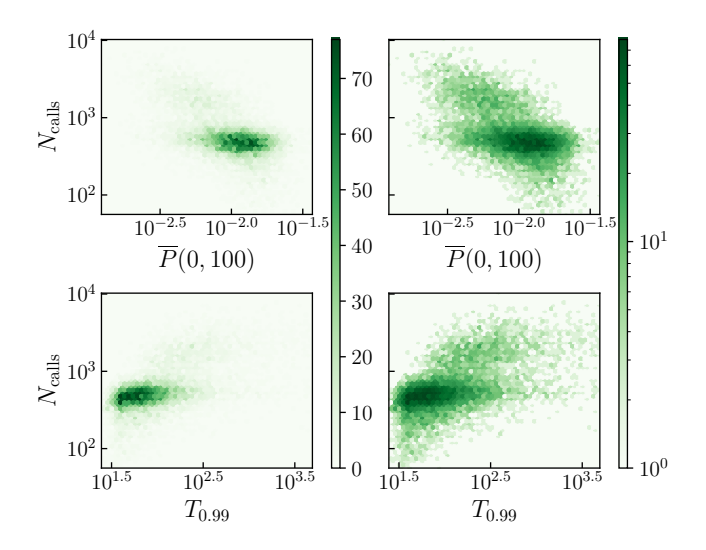


FIG. 6. Heatmaps of the number of problem calls  $N_{\rm calls}$  against the QW success probability  $\overline{P}(0,100)$  (top) and the AQC duration  $T_{0.99}$  (bottom) on log-log axes for typical instances with n=15 variables. The bottom plots exclude 132 instances for which  $T_{0.99}$  was not successfully calculated. The left column shows the heatmaps with a linear colour scale, and the right column shows the same distributions with a logarithmic colour scale, where the value for each cell has been increased by one to remove the zeros. Visually, some correlation can be seen in both distributions. The Spearman's rank correlation coefficient is  $\approx -0.47$  for the top-left plot and  $\approx 0.52$  for the bottom-left plot.

and classical algorithm, as opposed to the two quantum algorithms that we are considering. This does not rule out the possibility of a better performance attained from other forms of (hybrid) quantum algorithms.

We note that since different classical algorithms will have varying levels of correlation with each other, our measure of "classical hardness" cannot be extended to represent hardness for classical algorithms as a whole, since such a thing does not exist. However, the fact that some correlation exists between hardness for the quantum algorithms and hardness for MixBandB is still interesting, as it indicates that there are some characteristics of instances which make them typically harder for both the quantum algorithms and some "good" classical algorithms. Further work is required to find out if there are other good classical algorithms with lower levels of correlation with the quantum algorithms.

#### C. Satisfiable instances

Satisfiable instances of MAX 2-SAT are easy to solve classically because the optimal solution can be found with a 2-SAT solver, and 2-SAT is known to be in P; a linear time algorithm for 2-SAT was found in [33], which is based on finding the strongly connected components of the problem's implication graph. Some of the typical instances that we are analysing are satisfiable, the proportion of which decreases with n. A good classical MAX SAT solver will take advantage of this to solve satisfiable instances efficiently, for example by calling a 2-SAT solver at the start of the algorithm. However, since the quantum algorithms we are studying don't explicitly check for the satisfiability of formulae, it is unclear whether they will find satisfiable instances easy. In this subsection, we analyse the hardness of satisfiable instances for QW and AQC and discuss the implications of this for a hybrid

The plots in the top row of Fig. 7 show the approximate probability density of the QW success probability  $\overline{P}(0,100)$  for satisfiable and unsatisfiable instances with n=5 and n=15 variables. The median value of each distribution is indicated by a vertical line. We find that the median  $\overline{P}(0,100)$  for satisfiable instances is larger than for unsatisfiable instances at n = 15, but at n = 5the satisfiable instances have a smaller median  $\overline{P}(0, 100)$ than the unsatisfiable instances. This indicates that QW finds satisfiable instances easier on average except in the case of very small n, although even at n=5 the very hardest instances still tend to be unsatisfiable. We note that the long tail of hard instances cannot be as easily identified in the top-right plot as it can in Fig. 2, which is because we are using a linear x-axis in Fig. 7 and QW hardness is inversely proportional to  $\overline{P}(0, 100)$ . The tail of hard instances can be clearly seen in both of the n=15 distributions when plotting for  $1/\overline{P}(0,100)$  or using a logarithmic x-axis.

In practice, the satisfiable instances are easier for QW than what can be inferred from the plots in Fig. 7. This is due to the fact that the QW success probability is generally much less than 1, so repeat runs are needed to increase the probability of finding the optimal solution. From Eq. (12), we can see that each unsatisfied clause adds an energy contribution of 1. Therefore, by

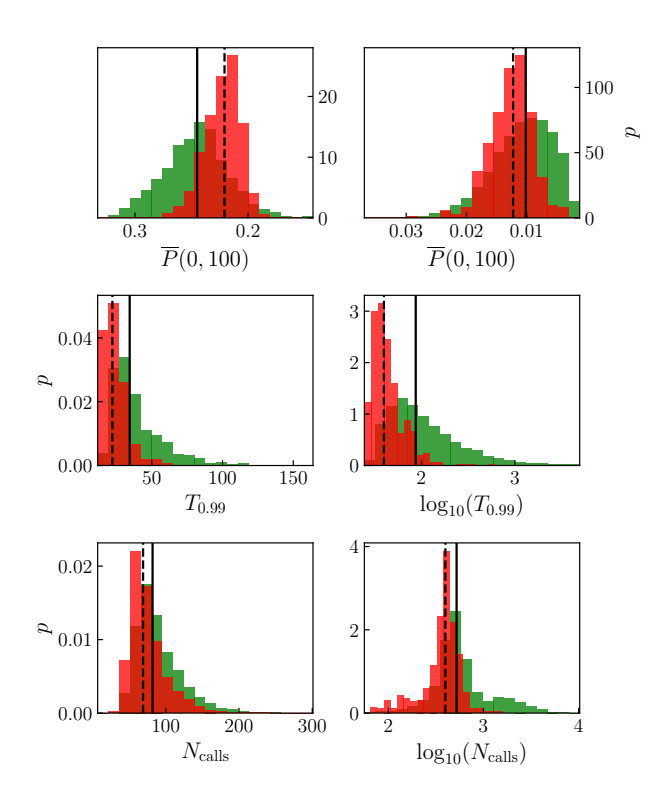


FIG. 7. Histograms of the approximate probability density p of the QW success probability  $\overline{P}(0,100)$  (top row), AQC duration  $T_{0.99}$  (middle-left), logarithm of  $T_{0.99}$  (middle-right), MixBandB calls  $N_{\rm calls}$  (bottom-left), and logarithm of  $N_{\rm calls}$  (bottom-right) for typical satisfiable (red) and unsatisfiable (green) MAX 2-SAT instances with n=5 variables (left column) and n=15 variables (right column). The top row of plots have reversed x-axes so that instance hardness increases from left to right for all plots. Median values of the distributions are indicated by dashed lines for satisfiable instances and solid lines for unsatisfiable instances.

measuring the energy of the final state, or by classically evaluating the formula with the solution given by QW, we can efficiently determine how many clauses are left unsatisfied by the corresponding solution. If the optimal solution of a satisfiable instance is found, it would become immediately obvious that there are no more clauses that can be satisfied, so repeat runs would no longer be necessary. For unsatisfiable instances, we cannot be certain that we have found an optimal solution based on the information gained from QW alone, so there will typically be "wasted" runs conducted even after finding the optimal solution. The number of extra runs depends on the specific strategy used to determine when to stop doing repeats. There has been previous work on applying sophisticated methods of determining the stopping point to quantum annealing [34].

The middle row of Fig. 7 shows the approximate probability density of the AQC duration  $T_{0.99}$  for typical satisfiable and unsatisfiable instances with n=5 variables, and similarly for the approximate probability density of

the logarithm of  $T_{0.99}$  for n=15. The satisfiable instances have shorter median durations than the unsatisfiable instances for both n=5 and n=15, indicating that AQC finds these problems easier on average. Since AQC achieves a high success probability in a single run, we do not need to do repeat runs as in the case for QW, so these plots are a good representation of the difference in AQC hardness between satisfiable and unsatisfiable instances. The bottom row of Fig. 7 shows similar results for the MixBandB algorithm, which like the quantum algorithms does not check for satisfiability. Satisfiable instances are found easier on average, but the distributions for satisfiable and unsatisfiable instances overlap.

The significant overlap between the distributions of satisfiable and unsatisfiable instances in Fig. 7 either imply that QW and AQC do not find satisfiable instances as easy as the best classical algorithms, or that a large fraction of the unsatisfiable instances at these problem sizes are just as easy as the satisfiable instances, which are in P. To attempt to determine which of these two cases is true, we can check whether the hardness of satisfiable instances scales polynomially for the quantum algorithms, which would indicate that QW and AQC can solve them efficiently.

We plot the scaling of the median QW success probability and AQC duration with n for satisfiable and unsatisfiable instances on log-linear and log-log axes in Fig. 8. An exponential scaling would fit better to a straight line on log-linear axes, whereas a polynomial scaling would have a better linear fit on log-log axes. For QW, we can see that the log-linear axes produce better fits for both sets of instances, meaning that the median of  $\overline{P}(0,100)$  appears to scale exponentially with n for both satisfiable and unsatisfiable instances. For AQC, it is unclear which fits are better. We note that these results cannot be used to make statements about the form of the scalings with certainty, as the problem sizes are very small compared to practically relevant instances and the scalings may change at larger sizes.

Given the linear worst-case scaling of good classical 2-SAT solvers and the apparent exponential scaling of QW (and potentially AQC) on satisfiable instances, we can conclude that a classical algorithm should most likely be used to efficiently check the satisfiability of instances at the start of any hybrid algorithm involving QW and/or AQC, as these instances cannot be solved as efficiently by the quantum algorithms. This will speed up the time to solution for satisfiable instances while only contributing a linear overhead to the run time for unsatisfiable instances. An added benefit of this approach is that instances with exactly one clause that is unsatisfied by an optimal assignment can be solved faster by QW. This is because by running a classical 2-SAT solver in advance, it would become known when a formula is unsatisfiable and that any assignment satisfying all but one clause is optimal. Therefore, there would be no need for repeat runs of QW after an optimal solution is found, for the same reasons as we mentioned for satisfiable instances.

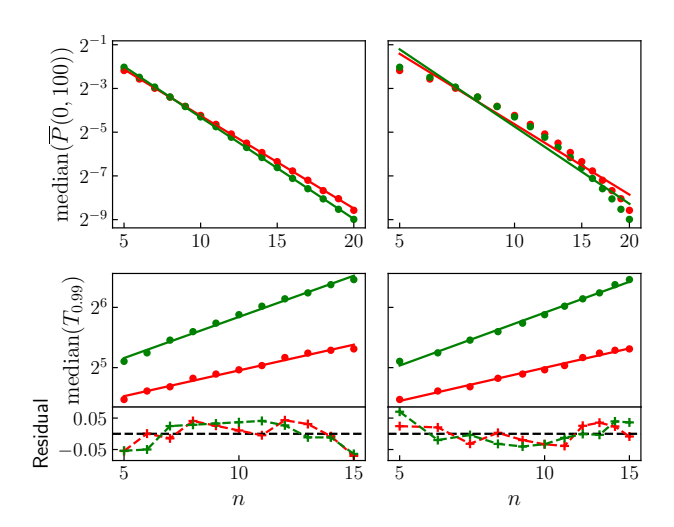


FIG. 8. The top row shows plots of the median QW success probability  $\overline{P}(0,100)$  for all satisfiable (red) and unsatisfiable (green) typical instances against the number of variables n. The top-left plot uses log-linear axes, and the top-right plot uses log-log axes. Linear fits are shown for both the satisfiable and unsatisfiable instances. The bottom row is the same as above, but for the AQC duration  $T_{0.99}$ . Residuals, which are calculated logarithmically as  $\log_2(\text{median}(T_{0.99})) - \log_2(y(n))$ , where y(n) is the corresponding fit, are also shown in the bottom row for both the satisfiable (red) and unsatisfiable (green) instances.

# V. CONCLUSIONS

We have examined both the relative hardness of different instances and the correlation in hardness for a selection of both classical and quantum algorithms. These include algorithms that behave in conceptually different ways, for example quantum walk, which relies on many repeats with a relatively low success probability, versus adiabatic quantum computing, which succeeds with a high probability after a single run. We have found that while there is some correlation in MAX 2-SAT instance hardness between methods, the correlation seems weak enough that a strategy of attempting multiple algorithms in parallel is viable and likely to be desirable in real computation. We also note unique features of specific strategies, for example the performance of the very hardest instances for AQC is drastically worse than for more "typical" problems, much more so than for quantum walk. This catastrophic failure suggests that a "stand alone" adiabatic strategy without attempting others in parallel is likely to be particularly undesirable. We further find that while the performance of quantum algorithms is generally better for specifiable problems (which can be solved efficiently classically), these problems are still not solved trivially by either of the quantum algorithms. This strongly suggests that first performing a classical check for satisfiability is useful. In a sense, attempting different algorithms in parallel can be seen as the most trivial sense of having a hybrid algorithm. If the algorithms are classical and quantum then it is a hybrid quantum-classical algorithm, but there can also be hybrids between two quantum algorithms, such as AQC and QW. While not the topic of this paper, the fact that even such simple hybrid methods are desirable bodes well for more complicated methods of combining algorithms that are likely to lead to further gains, for example pre-annealing in [10] as a quantum-quantum algorithm, or various biasing and reverse annealing techniques [35] as examples of quantum-classical hybrids.

The correlations do suggest that while attempting multiple different algorithms in parallel is likely to be fruitful, there is also likely a more fundamental sense of hardness in terms of being resistant to being solved by any algorithm, quantum or classical. Furthermore, the double peaked nature of many of the distributions of effort required for problems suggests that the transition toward being hard as problems scale toward the large size limit is not simple, at least not in the case of MAX 2-SAT. While this behaviour is partially explained by the difference between satisfiable and unsatisfiable instances, this appears not to be the whole story, because there is sig-

nificant overlap between the two in terms of hardness. While we have made significant steps in understanding relative problem hardness over different algorithms at sizes relevant for exhaustively simulated quantum computing, there is still much work to be done to fully understand this important topic which underlies many numerical studies.

#### ACKNOWLEDGMENTS

We thank the members of Algorithms and Complexity in Durham for helpful discussions. NC and VK were supported by EP/L022303/1 and impact acceleration funding associated with this grant. NC was supported by EP-SRC fellowship EP/S00114X/1. PM was supported by EPSRC Doctral training funds awarded to Durham University (EP/T518001/1). AC was funded by UKRI EPSRC Grant No. EP/L016524/1 via the Imperial College London Centre for Doctoral Training in Controlled Quantum Dynamics, and the EPSRC UK Quantum Technology Hub in Computing and Simulation (EP/T001062/1).

- A. Callison, N. Chancellor, F. Mintert, and V. Kendon, New Journal of Physics 21, 123022 (2019).
- [2] J. Roland and N. J. Cerf, Phys. Rev. A 65, 042308 (2002).
- [3] N. Shenvi, J. Kempe, and K. B. Whaley, Phys. Rev. A 67, 052307 (2003).
- [4] J. G. Morley, N. Chancellor, S. Bose, and V. Kendon, Phys. Rev. A 99, 022339 (2019).
- [5] E. Crosson, E. Farhi, C. Y.-Y. Lin, H.-H. Lin, and P. Shor, Different Strategies for Optimization Using the Quantum Adiabatic Algorithm (2014), arXiv preprint quant-ph/1401.7320.
- [6] E. Farhi and S. Gutmann, Phys. Rev. A 58, 915 (1998).
- [7] T. G. Wong and D. A. Meyer, Phys. Rev. A 93, 062313 (2016).
- [8] E. Farhi, J. Goldstone, S. Gutmann, and M. Sipser, Quantum Computation by Adiabatic Evolution (2000), arXiv preprint arXiv:quant-ph/0001106.
- [9] M. Born and V. Fock, Zeitschrift für Physik 51, 165 (1928).
- [10] A. Callison, M. Festenstein, J. Chen, L. Nita, V. Kendon, and N. Chancellor, PRX Quantum 2, 010338 (2021).
- [11] MaxSAT Evaluations, https://maxsat-evaluations.github.io/ (2022), [Online; accessed 14-June-2022].
- [12] SAT Competition, https://satcompetition.github.io/(2022), [Online; accessed 14-June-2022].
- [13] E. Clarke, D. Kroening, and F. Lerda, in *International Conference on Tools and Algorithms for the Construction and Analysis of Systems (TACAS 2004)* (Springer, Barcelona, Spain, 2004) pp. 168–176.
- [14] F. Ivančić, Z. Yang, M. K. Ganai, A. Gupta, and P. Ashar, Theoretical Computer Science 404, 256 (2008).
- [15] H. Kautz, B. Selman, and M. Hill, in European Conference on Artificial Intelligence (Vienna, Austria, 1992) pp. 359–363.

- [16] J. Rintanen, Artificial Intelligence 193, 45 (2012).
- [17] S. Safarpour, H. Mangassarian, A. Veneris, M. H. Liffiton, and K. A. Sakallah, in *Formal Methods in Computer Aided Design (FMCAD '07)* (IEEE, 2007) pp. 13–19.
- [18] Y. Chen, S. Safarpour, J. Marques-Silva, and A. Veneris, IEEE Transactions on Computer-Aided Design of Integrated Circuits and Systems 29, 1804 (2010).
- [19] D. Coppersmith, D. Gamarnik, M. T. Hajiaghayi, and G. B. Sorkin, Random Structures & Algorithms 24, 502 (2004).
- [20] W. Fernandez de la Vega, Theoretical Computer Science 265, 131 (2001).
- [21] S. Santra, G. Quiroz, G. Ver Steeg, and D. A. Lidar, New Journal of Physics 16, 10.1088/1367-2630/16/4/045006 (2014).
- [22] P. Austrin, in Proceedings of the thirty-ninth annual ACM symposium on Theory of computing (STOC '07) (ACM Press, San Diego, California, USA, 2007) p. 189.
- [23] G. van Rossum and F. L. Drake Jr, *Python tutorial* (Centrum voor Wiskunde en Informatica, 1995).
- [24] C. R. Harris, K. J. Millman, S. J. van der Walt, R. Gommers, P. Virtanen, D. Cournapeau, E. Wieser, J. Taylor, S. Berg, N. J. Smith, et al., Nature 585, 357 (2020).
- [25] P. Virtanen, R. Gommers, T. E. Oliphant, M. Haberland, T. Reddy, D. Cournapeau, E. Burovski, P. Peterson, W. Weckesser, J. Bright, et al., Nature Methods 17, 261 (2020).
- [26] J. D. Hunter, Computing in Science & Engineering 9, 90 (2007).
- [27] J. Gray, Journal of Open Source Software 3, 819 (2018).
- [28] E. Hairer, S. P. Nørsett, and G. Wanner, Solving Ordinary Differential Equations I: Nonstiff Problems, Vol. 8 (Springer, 1993).
- [29] A. Callison, Continuous-time Quantum Computing,

- Ph.D. thesis, Imperial College London (2021).
- [30] P. W. Wang and Z. J. Kolter, Proceedings of the AAAI Conference on Artificial Intelligence **33**, 1641 (2019).
- [31] P.-W. Wang, W.-C. Chang, and J. Z. Kolter, The Mixing method: low-rank coordinate descent for semidefinite programming with diagonal constraints (2017), arXiv preprint arXiv:1706.00476.
- [32] D. S. Steiger, T. F. Rønnow, and M. Troyer, Physical Review Letters 115, 1 (2015).
- [33] B. Aspvall, M. F. Plass, and R. E. Tarjan, Information Processing Letters 8, 121 (1979).
- [34] W. Vinci and D. A. Lidar, Phys. Rev. Applied 6, 054016 (2016).
- [35] N. Chancellor, New Journal of Physics 19, 023024 (2017).